

THS (1701/)



This is to certify that the

thesis entitled TRIGEMINAL EFFERENT PROJECTIONS TO AUTONOMIC NUCLEI IN RAT SPINAL CORD: A LIGHT AND ELECTRON MICROSCOPIC STUDY

presented by

LISA ANN BELT

has been accepted towards fulfillment of the requirements for

M.S. degree in Anatomy

William M. Jell-Ph D.

Major professor

Date 12-16-96

MSU is an Affirmative Action/Equal Opportunity Institution

0-7639

LIBRARY Michigan State University

PLACE IN RETURN BOX to remove this checkout from your record. TO AVOID FINES return on or before date due.

DATE DUE	DATE DUE	DATE DUE

MSU Is An Affirmative Action/Equal Opportunity Institution ctcirc/datedus.pm3-p.1

TRIGEMINAL EFFERENT PROJECTIONS TO AUTONOMIC NUCLEI IN RAT SPINAL CORD: A LIGHT AND ELECTRON MICROSCOPIC STUDY

By

LISA ANN BELT

A THESIS

Submitted to
Michigan State University
in partial fulfillment of the requirements
for the degree of

MASTER OF SCIENCE

Department of Anatomy

1996

ABSTRACT

TRIGEMINAL EFFERENT PROJECTIONS TO AUTONOMIC NUCLEI IN THE RAT SPINAL CORD: A LIGHT AND ELECTRON MICROSCOPIC STUDY

By

LISA ANN BELT

Anterograde transport of Phaseolus vulgaris leucoagglutinin (PHA-L) was used to determine the overall morphology, distribution and synaptic relations of efferent axons originating from neurons in dorsomedial (DM) and ventrolateral (VL) subdivisions of rat trigeminal nucleus oralis (Vo) and terminating in the sympathetic interomediolateral cell column (IML) throughout the thoracic spinal cord. Light microscopical findings reveal that from cells in each subdivision two morphologically distinct types (Types I and II) of efferent axons project bilaterally to IML. Type I efferents are a direct continuation of parent axons in the lateral funiculus. They enter IML dorsally after sending branches into lamina V. Within IML these axons branch into several medially directed thin terminal strands containing up to six boutons. Parent fibers of Type II efferents enter the thoracic ventral horn from the anterior funiculus and proceed dorsally through lamina VIII, IML, and laminae IV and V. In IML each parent axon gives rise to one or two collateral branches which terminate into thin terminal strands containing one to four boutons. Electron microscopic analyses reveal that the majority of boutons from Type I efferents

are filled with closely packed agranular spherical synaptic vesicles among which are scattered several dense core vesicles. These axonal endings form asymmetrical to intermediate synaptic junctions on large diameter (2.0 - 5.0 µm) dendritic shafts. Boutons of Type II efferents are filled with a single population of agranular spherical synaptic vesicles. These axonal endings form asymmetrical to intermediate junctions on the neuronal cell bodies as well as on large and small diameter (1.0 -2.0 µm) dendritic shafts. Within IML the majority of cell bodies and dendrites receiving Vo input are thought to be preganglionic sympathetic neurons. The results of this study suggest that sensory input from orofacial regions innervated by the trigeminal nerve may have a significant influence on sympathetic outflow to the entire body.

DEDICATION

To my family, Phil, Sandi and Scott Belt and my future husband, Douglas Lupini

ACKNOWLEDGEMENT

I would like to express my thanks and appreciation to my advisor Dr. William M. Falls for his patience, support and guidance throughout my graduate studies. I would also like to thank the members of my graduate committee: Drs. Irena Grofova, Ralph Pax and Arthur Weber for their support and guidance.

I would like to extend my gratitude to the faculty and the staff of the Department of Anatomy as well as my fellow graduate students for their friendship, support and encouragement.

Many individuals are remembered for their support and encouragement, however the love of my family and friends helped me achieve my goals.

TABLE OF CONTENTS

st of Figures	
obreviations	i
troduction	
aterials and Methods	
esults	
scussion	,
gures	ı
bliography	

LIST OF FIGURES

1.	PHA-L Injection Sites
2.	Type I Efferent Axon Terminal Arbors
3.	Type II Efferent Axon Terminal Arbors
4.	Light Micrographs of Type I and Type II Efferent Axon Terminal Arbors25
5.	Electron Micrographs of the Cytology and Synaptic Relations of a Type I Efferent Axonal Ending
6.	Electron Micrograph of the Cytology and Synaptic Relations of a Type II Efferent Axonal Ending
7.	Electron Micrograph of a Type II Efferent Parent Axon
8.	Electron Micrograph of the Cytology and Synaptic Relations of Type II Efferent Axonal Ending
9.	Electron Micrograph of the Cytology and Synaptic Relations of Type II Efferent Axonal Ending

ABBREVIATIONS

AF anterior funiculus

AMB nucleus ambiguus

AP astrocytic process

b bouton

BZ border zone subdivision

D dendrite

DAB 3,3' diaminobenzidine subdivision

dcv dense core vesicle

DH dorsal horn

DM dorsomedial subdivision

HRP horseradish peroxidase

IML interomediolateral cell column

IS injection site

LF lateral funiculus

MDH medullary dorsal horn

PF posterior funiculus

PHA-L phaseolus vulgaris leucoagglutinin

RT room temperature

S soma

SVT spinal trigeminal tract

TBS-TX tris buffered saline with triton X

TS terminal strand

VII facial motor nucleus

VH ventral horn

VL ventrolateral subdivision

Vo trigeminal nucleus oralis

Vo-TS trigeminal nucleus oralis- trigeminospinal

Vi trigeminal nucleus interpolaris

INTRODUCTION

Clinical outcomes from mechanical manipulation of the head (noxious and innocuous) using osteopathic craniosacral techniques support the existence of efferent projections from neurons in sensory trigeminal nuclei receiving these mechanical inputs via axons of primary trigeminal neurons to autonomic centers in the brainstem and spinal cord (26). Autonomic responses, both sympathetic and parasympathetic to stimulation of trigeminal primary afferents include: sweating on the brow, pupillary changes (constriction and/or dilation), nausea, vomiting, increases and decreases in the heart rate, diving reflex, flushing of the skin and feelings of anxiety, to name a few. Knowledge of the circuitries underlying the myriad of autonomic responses are essential if one is to understand the functional consequences of osteopathic craniosacral manipulative techniques. The purpose of the present investigation is to extend previous studies (24,46,53) and to provide new anatomical evidence for the existence of a trigeminospinal tract linking neurons in trigeminal nucleus oralis (Vo) with the preganglionic sympathetic neurons in the thoracic interomediolateral cell column (IML).

Previous studies (18,19, 21,22,23) have shown that each of the three subdivisions of rat Vo; dorsomedial (DM), ventrolateral (VL), and border zone (BZ); received functionally and morphologically distinct groups of primary and non-primary afferent axons which directly influence second order Vo projection neuron activity. Primary afferents convey to Vo mechanoreceptive and nociceptive information from oral and

perioral areas as well as mechanoreceptive input from the face and oral cavity. Efferent outflow from each Vo sudivision is provided by axons of second order Vo projection neurons which affect synaptic activity in many target areas along the neuraxis. The existence of trigeminospinal projections, originating from neurons in all portions of the spinal trigeminal nucleus (SVN): Vo, trigeminal nucleus interpolaris (Vi), and medullary dorsal horn (MDH, trigeminal nucleus caudalis) have been established by previous investigations in rats (7, 9, 20, 34, 46, 47), cats (7, 8, 14, 29, 32, 37, 38, 39, 56), dogs (14), hamsters (6), monkey (9) and opossum (10, 16). Retrograde studies of Vo trigeminospinal (Vo-TS) projection neurons situated in VL have shown bilateral projections along the entire length of the spinal cord (34, 46) and their termination in dorsal and ventral horns as well as intermediate gray (lamina VII) suggest that they influence the activity of somatosensory relay neurons, somatic motor neurons, and preganglionic autonomic motoneurons as well as interneurons. Based on retrograde transport studies, rat VL has been shown to contain large multipolar cells that innervate cervical, thoracic, and lumbar spinal cord levels (53, 56). Anterograde studies using Phaseolus vulgaris leucoagglutinin (PHA-L) have confirmed projections of Vo neurons along the entire length of the spinal cord (53). Terminal arbors of axons of Vo-TS projection neurons were found in dorsal and ventral horn laminae as well as thoracic and sacral IML. Numerous Vo-TS axons were observed following VL injections. However, a considerably higher density of fibers was seen following injections into DM. Previous data (53) show that two morphologically distinct types of efferent fibers emanate from DM and VL neurons and teminate in IML of the thoracic cord.

In the present study PHA-L was injected into Vo with Dm and VL as the principle targets. Identification of Vo injection sites as well as the overall morphology of Vo-TS efferent axons terminating in thoracic IML were analyzed using the light microscope. The overall axonal morphology was compared to those observed in previous studies (53) in order to determine fiber type. Once the efferent fiber types were identified at the light microscopic level they were then examined under the electron microscope in order to determine their cytology and synaptic relations with neuronal elements in thoracic IML.

MATERIALS AND METHODS

Eighteen male Sprague-Dawley albino rats (200-300g) were anesthetized with intaperitoneal injection of sodium pentobarbitol and placed in a stereotaxic apparatus. The cranium was opened unilaterally through the occipital bone and the dura incised.

Ionotophoretic injections were made into DM and VL of Vo unilaterally using glass micropipettes (inside tip diameter 20-30 μm) filled with 2.5% PHA-L (Vector Labs) in 0.05M sodium phosphate buffered (pH 7.4) saline. Micropipette electrodes were lowered into DM and VL passing through the cerebellum at an angle of approximately 90° with respect to the horizontal plane. Stereotaxic coordinates for electrode placement used in this study were determined in previous PHA-L studies of Vo efferents to rat spinal cord (53, 54). Ionotophoretic parameters were set up to use a current of 5 μA provided by an alternating current source (Midguard, Transkinetictics Model CS3) which was applied at intervals of 7 seconds on and 7 seconds off for 45-60 minutes.

After postinjection periods of 10-14 days the animals were deeply anesthetized and perfused transcardially with two solutions at 4°C. The first solution consisted of 250ml of 150mM acatate buffer (pH 6.5) containing 4% paraformaldehyde. The second solution consisted of 750ml 65mM borate buffer (pH 9.5) containing 4% paraformaldehyde and 0.05% gluteraldehyde. After perfusion the brain and spinal cord were removed, post-fixed overnight at 4°C in the last perfusiate buffer and cut serially into 20-30um coronal sections using and Oxford Vibratome into tris buffered saline (TBS, pH 7.6) at room temperature

(RT). After three rinses in TBS with 0.04% Triton X-100 (TBS-TX) at RT sections were placed in a solution of normal rabbit serum in TBS-TX for 30 minutes at RT and rinsed once in TBS-TX at RT. Sections were then incubated for 24-48 hours in anti-PHA-L (1:2000; Vector Labs) diluted in TBS-TX at 4 C. No labeling was observed when the anti-PHA-L was eliminated. To visualize the PHA-L, sections were processed with the avidin- biotinylated HRP ABC technique using Vecastain ABC Kit (Vector Labs). Final peroxidase reactions were performed with DAB (100mg in 100ml 0.15M TBS). The 100ml DAB solution also contained 40mg ammonium chloride, 200mg glucose oxidase and 38mg Imidozole. Sections were incubated in the DAB solution for 45-60 minutes. After they were immunoreacted the sections were cleared through a graded series of glycerol concentrations (20, 40, 60, 80, and 100% for 5 minutes each), placed on glass slides in 100% glycerin and coverslipped.

Detailed light microscopic evaluations of each section through Vo and the rostrocaudal extent of thoracic IML were undertaken in order to determine the injection site in Vo as well as the overall course and distribution, organization and morphology of Vo-TS efferent axons and their terminal arbors in thoracic cord. Sections not containing isolated or completely labeled axons suitable for electron microscopic evaluations were rehydrated through a descending series of glycerin concentrations (80, 60, 40, and 20%), mounted on glass slides, counterstained with cresyl violet and coverslipped. All light microscopic evaluations were performed with a Leitz laborlux 12 microscope fitted with a drawing tube. Detailed drawings of PHA-L labeled Vo-TS efferent axons and their terminal arborizations in IML to be taken for electron microscopic evaluation were made

using 100X oil immersion objective lens at a magnification of 1250X. Photographs to illustrate specific morphological features of Vo-TS axons, such as their diameters, were also taken.

Coronal sections through thoracic IML containing isolated and completely labeled Vo-TS efferent axons were processed for electron microscopy. The IML and surrounding area were dissected out of each section and rehydrated through a descending series of glycerol concentrations (80, 60, 40, and 20% for 5 minutes each) before being osmicated in 2% osmium tertoxide, rinsed in distilled water and stained en bloc in 1% aqueous uranyl acatate and embedded in Marglas. Sections through thoracic IML containing PHA-L labeled fibers and their terminals were thinly sectioned (many in series). Sections were oriented so that as much as possible of the axons would be cut transversely. Sections were mounted on Fromvar-coated grids, stained with lead citrate and examined in an electron microscope.

Electron micrographs from sections through light microscopically identified PHA-L labeled Vo-TS efferent axons and their terminal arbors in thoracic IML were examined to observe their size, shape and relationship to other neuronal structures (soma, dendrites and axons) as well as their cytoplasmic structure. Labeled Vo-TS efferent axonal endings were classified as to their size and shape as well as the size, shape and compactness of their synaptic vesicles. The type of synaptic junction made with postsynaptic dendrites and neuronal cell bodies was also classified. Ninety-six labeled axonal endings were examined in this study and classified into two morphologically distinct types Type I (56 endings) and Type II (40 endings). Diameters of postsynaptic

dendrites were also measured. Dendritic diameters were detremined from profiles cut either longitudinally or transversely in which neurotubule membranes were clearly visible and properly oriented.

RESULTS

Injection Sites

PHA-L was injected unilaterally into Vo with the middle of DM and VL as the principal targets (Figure 1). Areas containing densely filled neurons within DM and VL were considered effective zones which had efferents projections originating from them. Anterograde axonal labeling was seen following PHA-L deposits into DM and VL with minimal spillover into adjacent areas. Densely filled neurons were never observed in adjacent areas following PHA-L injections into DM and VL.

In this study ten successful experiments resulted in the bulk of the PHA-L being deposited into DM. Two of the brains are used to illustrate representative injection sites (Figure 1A, schematically, and Figures 1B, C photographically) from the ten studied. The DM injection site depicted in Figure 1B was situated in the middle of DM. It was confined to the subdivision with some spillover into dorsal BZ. The injection site, as measured in transverse serial sections, extended 1180 µm rostrocaudally, 910 µm dorsoventrally and 1180 µm mediolaterally. The second DM injection site as shown in Figure 1C also was confined to the subdivision with some spillover into dorsal VL. It measured 720 µm rostrocaudally, 1230 µm dorsoventrally and 1090 µm mediolaterally. Eight successful experiments resulted in PHA-L being deposited principally into VL. One brain is used to illustrate a VL injection site (Figure 1A, schematically and Figure 1D, photographically). This injection site filled VL and adjacent BZ and spread into the spinal

trigeminal tract (SVT). It did not extend into DM or dorsal BZ. This injection site is representative of the eight injection sites studied and the results from it are reported in this study. The injection site, as measured transversely in serial sections extended 1100um dorsoventrally, 1200 μm rostrocaudally, and 1000 μm mediolaterally. The combination of these three injection sites completely filled DM and VL (Figure 1A) and allowed for accurate analysis of Vo-TS efferent projections to thoracic IML.

Light Microscopy

Following injections targeted to DM and VL, PHA-L labeled parent Vo-TS axons and their terminal arbors were visible throughout the rostrocaudal length of the thoracic spinal cord. Several descending fibers terminated in the IML bilaterally. The overall morphology and their manner of termination in IML allows for the classification of these Vo-TS efferent axons from both subdivisions into two types; Type I and Type II. These two types are identical to those found in a previous PHA-L study (53, 54).

Terminal arbors of Type I Vo-TS efferent axons (Figures 2, 4) are a direct continuation of their parent fibers (1.0 to 2.0 µm in diameter) in the lateral funiculus. The parent axons enter IML dorsally after sending branches into lamina V. Upon entering the IML parent fibers branch into several medially directed thin terminal strands (0.5 to 1.0 µm in diameter) which are confined to IML (Figure 2B). Along the terminal strands are one to six irregularly spaced boutons en passant and terminal boutons (Figure 2C, D, 4). These spherical to elliptical-shaped boutons measure 1.5 to 5.0 µm in diameter.

Parent fibers (3.0 to 5.0 µm in diameter) of Type II Vo-TS efferent axons enter the thoracic ventral horn from the anterior funiculus (Figure 3B). They proceed dorsally through the lateral aspect of ventral horn laminae VIII and IV, pass through IML, and proceed into dorsal horn laminae IV and V. In IML each parent fiber gives rise to one or two collateral branches which undergoes secondary branching (Figures 3B-D). From these branches emerge thin terminal strands measuring 0.5 to 1.0 µm in diameter (Figures 3D, 5). Some terminal strands emanate directly from the parent fiber (Figure 3C). Along a terminal strand are one to four irregular spaced boutons en passant with a bouton at the end of each terminal strand. Boutons measure 1.5 to 5.0 µm in diameter and display spherical to elliptical shapes. The terminal axonal arbor is oval in shape and is confined to IML (Figure 3B).

Electron Microscopy

Electron microscopic analysis of PHA-L labeled parent fibers of Type I and Type II Vo-TS efferent axons terminating in thoracic IML show that they are thinly myelinated (Figure 7). The myelin sheaths of both types of parent axons range from 0.1 to 1.5 μm in thickness. The terminal strands of both types of Vo-TS efferents are unmyelinated (Figure 6, 9). These findings substantiate the light microscopical findings for the diameter of parent axons and terminal strands of both types of Vo-TS efferents terminating in thoracic IML.

Within the thoracic IML neuropil axonal endings of both Types I and Type II Vo-TS are found singly (Figures 5,6,8,9). However, the endings of each type are

structurally different and can be distinguished form each other on the basis of their cytology and synaptic relations (Figure 5,6,8,9).

The majority of the endings of Type I Vo-TS efferent axons have an elongated appearance and display either a scalloped (Figures 5A, B) or smooth contour (Figures 6A, B). They are filled with closely packed agranular spherical synaptic vesicles (40-60 nm in diameter) among which are scattered several spherical dense core vesicles (85-100 nm in diameter; Figure 6B). These axonal endings form single or multiple asymmetrical to intermediate synaptic junctions on a single dendritic shaft. These dendritic shafts measure 2.0 to 5.0 µm in diameter and contain some granular endoplasmic reticulum as well as neurofilaments, neurotubules, agranular endoplasmic reticulum and mitochondria (Figures 5, 6). Most endings of Type I Vo-Ts efferent axons are completely ensheathed by astrocytic processes except at their presynaptic membrane (Figures 5, 6).

Endings of Type II Vo-TS efferents axons present a dome-shaped appearance and are filled with a single population of agranular spherical (40-50 nm in diameter) synaptic vesicles (Figures 8,9). The synaptic vesicles aggregate at the one or two asymmetrical to intermediate synaptic junctions associated with each terminal. Endings of Type II Vo-TS efferents make synaptic contact with the cell bodies (Figure 8), large diameter dendrites (2.0 to 5.0 μm) as well as smaller dendritic shafts measuring 1.0 to 2.0 μm in diameter. A Type II ending synapses on a single dendritic shaft. Type II axonal endings along the same terminal strand have been observed to synapse on large as well as smaller diameter dendritic shafts. Type II terminals are ensheathed by overlapping astrocytic processes except at their presynaptic membrane (Figures 8,9).

DISCUSSION

Light Microscopy

The present anatomical study demonstrates that IML of rat thoracic spinal cord receives bilaterally terminal arborizations of two morphologically distinct types of Vo-TS efferent axons; Type I and Type II. These findings support and extend previous light microcopical analyses (55) by showing that both types of axons arise from neurons in DM as well as VL. The exact morphology of DM and VL neurons giving rise to Type I and Type II Vo-TS efferent axons innervating IML have yet to be determined but they are part of the structurally and functionally diverse neuronal populations making up DM and VL. Type I Vo-TS efferents enter IML from the lateral funiculus while Type II Vo-TS efferents traverse the anterior funiculus and enter IML after giving off collaterals in the ventral horn. Axons exiting the anterior and lateral funiculi and terminating in IML have been identified by Ramon Y Cajal (44) in Golgi preparations in the newborn mouse. The axons appear to display morphologies similar to Types I and II Vo-TS efferents described in this study as well as in previous PHA-L investigations (54). Taken together these data suggest that in the rat there are two separate efferent tracts, both originating from two different Vo subdivisions, that are involved in conveying orofacial sensory input to IML. By virtue of these connections with IML, Vo must play an important role in the expression of reflexes involved in the intergration of trigeminal and sympathetic systems.

Methodological Considerations

The anterograde PHA-L method, which labels the axons and their terminal arborizations by injecting PHA-L at sites which contain the parent cell bodies and dendrites, was used to identify the overall morphology, cytology and synaptic relations of Vo-TS efferent axons projecting from DM and VL to IML of rat thoracic cord. The uptake and transport of PHA-L appears only in the parent cell bodies and dendrites and not in fibers of passage, although in other neuronal systems retrograde transport of PHA-L as well as anterograde transport of lectin through fibers of passage have been demonstrated (12, 52). The PHA-L injection sites in this study were relatively small which allows for complete filling followed by detailed characterization of Vo-TS efferent axons and their terminal arbors at the light microscopic level as well as their cytology and synaptic relations at the electron microscopic level. Injection sites were only considered effective if they filled a significant portion of the nucleus with little spillover into surrounding areas and contained densely filled neurons. Extensive labeling has been thought to be the result of increased uptake secondary to axonal damage produced by the administration of PHA-L by a continuous current (not a pulse every 7 seconds). When using a small micropipette and pulsed current as was done in this study, the number of labeled Vo-TS efferent axons was low (49). The differences observed in the morphologies of Vo-TS efferent axons and their terminal arborizations in IML arose from cells located within DM and VL PHA-L injection sites and not from fibers of passage. In this study PHA-L labeled neurons were not observed in areas outside the boundaries of DM and VL which contained either no PHA-L reaction product or was only lightly stained.

Recognition of morphological features of the terminal axonal arbors of Vo-TS efferent axons at the light microscopic level shows the great advantage that the PHA-L method has over other anterograde techniques such as radioactive amino acids, horseradish peroxidase (HRP) or wheat germ agglutinin conjugated to HRP (WGA-HRP) and Golgi (25, 61). In this study the labeling presented by PHA-L allows for recognition of two morphologically distinct types of Vo-TS efferents innervating thoracic IML.

Electron Microscopy

The ultrastructure portion of this study indicates that the axonal endings of Types I and II Vo-TS efferents in thoracic IML display differences in their synaptic relations and cytology. Axonal endings of both types of Vo-TS efferents synapse on dendrites while axonal endings of Type II Vo-TS efferents also synapse on neuronal cell bodies. The majority of neurons in IML belong to sympathetic preganglionic neurons as determined in retrograde HRP studies in the cat (11), dog (43), and rat (48). In addition, sympathetic preganglionic cells have also been observed in the lateral funiculus and the middle region of the intermediate gray adjacent to IML in a variety of mammals (42). The Golgi studies of Ramon Y Cajal (44) in the newborn mouse provide insight into the overall morphology of these sympathetic preganglionic neurons. Those neurons whose cell bodies are situated within IML have dendritic fields confined primarily to the region while neurons whose cell bodies are located in either the lateral funiculus or the intermediate gray send dendritic branches into IML. When taken together the results of these studies, along with the findings in the present investigation, strongly suggest that the axonal endings of Types I

and II Vo-TS efferents are most likely synapsing on the dendrites and cell bodies of sympathetic preganglionic neurons. Within IML, axonal endings of Type I Vo-TS efferent axons make synaptic contact with large diameter dendrites while terminals of Type II Vo-TS efferents synapse on the same size dendrites as well as cell bodies and smaller diameter dendritic branches. Based on these findings axonal endings of Type I efferents are most likely synapsing on sympathetic preganglionic neurons confined to IML while terminals of Type II efferents are probably synapsing on these same neurons as well as sympathetic preganglionic whose cell bodies are in the lateral funiculus and the middle portion of the intermediate gray by way of connections with their smaller diameter dendritic branches projecting into IML. Without taking into account the density of each type of axonal ending synapsing on IML neurons, it would appear that the axonal endings of Type II Vo-TS efferents, with their placement along the entire length of dendritic shafts of IML neurons as well as the cell bodies, would have a more important role in controlling the activity of sympathetic preganglionic neurons in IML than would the terminals of Type I Vo-TS efferents which synapses only on large diameter dendrites of the same neurons. It has long been suggested that axonal endings that contain sphericalshaped agranular synaptic vesicles and establish asymmetrical to intermediate synaptic contacts (axonal endings of both Type I and II Vo-TS efferents) may be associated with an excitatory function (57,58). The fact that all of the synaptic contacts observed throughout this study are of this type may therfore indicate a preponderance of excitatory synaptic inputs impinging on sympathetic preganglionic neurons in IML from secondorder DM and VL neurons. In addition to spherical agranular synaptic vesicles, axonal

endings of Type I Vo-TS efferents also contain large dense core vesicles (> 80 nm in diameter). Although it is not possible to identify the neurotransmitter from the ultrastructural appearance of synaptic vesicles in the presynaptic terminal, large dense core vesicles have long been associated with neuroactive peptides within the central nervous system. The fact that they are found in the terminals of Type I Vo-TS efferents suggests that peptides may play an important role in the activation of IML preganglionic neurons by orofacial stimulation. Immunocytochemical studies (1) support this assumption by indicating that IML receives afferent input from axons stained for somatostatin and oxytocin. Neuropeptide somastatin-like activity has been illustrated (5) while substance P and Met-enkephalin reactivity have been observed (personal communication with R. Bowker) for neurons in DM and VL, the same subdivisions whose neurons give rise to Types I and II Vo-TS efferents terminating in the IML of this study.

Functional Considerations

Vo appears to have the strongest projection to the spinal cord of the three major subdivisions of the rat spinal trigeminal nucleus (24) and these projections arise from neurons in DM and VL subdivisions (54). Previous light and electron microscopical data have shown that DM and VL receive the terminal arbors of small myelinated (A) primary trigeminal axons (24, 55). Based on previous electrophysiological data, these A fibers most likely respond to light tactile and/or noxious stimuli from the orofacial region (4,17,27,28,29,33,40,45,50,51). Taken together these data suggest that DM and VL neurons are involved in the processing of orofacial pain and/or tactile input from small

myelinated primary trigeminal axons. Autoradiographic, degeneration, and anterograde transganglionic HRP transport studies in cat and rat agree that primary trigeminal axons terminating in Vo are somatopically organized (2,3,13, 30,31,35,36,41,59,60). By comparing locations of the rat DM and VL subdivisions to the regions of termination of primary afferent axons belonging to branches associated with each of the divisions of rat trigeminal nerve (2,13,31,35), it can be concluded that DM and VL would be receiving the terminal arborizations of primary trigeminal neurons innervating mandibular, maxillary, and ophthalmic orofacial receptive fields. From these data it appears that Types I and II Vo-TS efferents originating from second-order neurons in DM and VL are probably conveying to thoracic IML orofacial pain and/or tactile information from the entire peripheral receptive field of the trigeminal nerve. The importance of this assumption is that mechanical and/or noxious stimulation of the orofacial regions innervated by the trigeminal nerve probably have a marked influence on sympathetic outflow from IML of the thoracic cord.

The sympathetic portion of the autonomic nervous system, for the most part, is activated by exterorecptive inputs arriving by way of somatic primary afferent fibers (e.g. trigeminal primary afferent input). These inputs are initiated by favorable and unfavorable changes in the environment. Clinical outcomes from mechanical manipulation of the head (noxious and innocuous) using both intra- and extraoral techniques support existence of efferent projections fom Vo neurons, which receive these primary trigeminal mechanical inputs, to IML neurons in the thoracic spinal cord (26). Manual manipulations of the cranium can either alleviate observed symptoms or produce the onset of new symptoms.

Sympathetic reflex responses throughout the body to mechanical stimulation of trigeminal primary afferents include: sweating, pupillary dialtion, decreased salivation (dry mouth), vasoconstriction in the skin and viscera, increased blood pressure, feelings of anxiety, increased heart rate, decreased intestinal movements, contraction of vesical and rectal sphincters, deepened respiration, and increased blood flow to skeletal muscles, heart, lungs, and brain. The Vo projections to IML provide an important link in a pathway by which exteroreceptive primary trigeminal inputs from the orofacial region can contribute to the expressions of reflexes involved in the integration of the trigeminal and sympathetic systems throughout the body. Though the trigemino-sympathetic pathway, Vo may be the portion of the spinal trigeminal nucleus which participates in the manifestation of sympathetic responses which have been observed clinically following manual manipulations of the head.

Figure 1: PHA-L Injection Sites

Representative transverse sections (A-D) showing the location of Phaseolus vulgaris leucoagglutinin (PHA-L) injection sites in rat trigeminal nucleus oralis (Vo). A. Composite schematic drawing of the three injection sites shown photographically in B-D. B. A PHA-L injection site located in the dorsomedial subdivision of Vo (DM) and extending dorsally into the dorsal portion of the border zone subdivision of Vo (BZ) as well as a short distance ventrally into the dorsal portion of the ventrolateral subdivision of Vo (VL). C. A PHA-L injection site located in DM which extends into dorsal BZ as well as a short distance ventrally into dorsal VL. D. A PHA-L injection site located in VL completely fills the subdivision as well as adjacent BZ and the spinal trigeminal tract (SVT) but does not extend into DM or dorsal BZ. VII, facial motor nucleus: AMB, nucleus ambiguus.

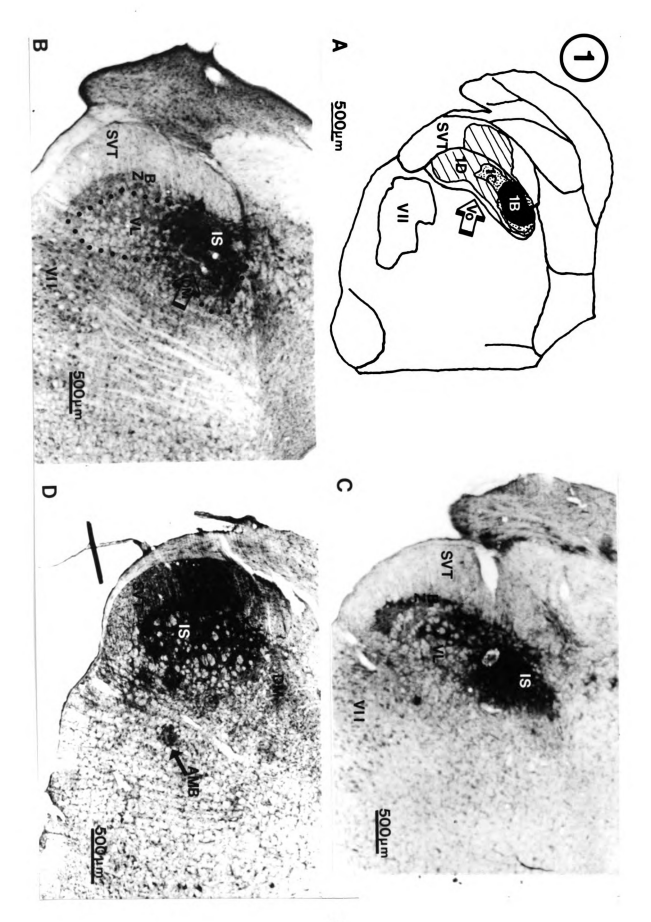


Figure 2: Type I Efferent Axon Terminal Arbors

Composite schematic drawings (A-D) showing the location and morphology of terminal arborizations of PHA-L labeled Type I Vo-trigeminospinal (TS) axons in the interomediolateral cell column (IML) of the thoracic spinal cord. A. Thoracic cord laminae. B. Terminal arborizations in IML of a Type I Vo-TS axon. The parent fiber enters the IML dorsally from the lateral funiculus (LF) after sending a branch into Lamina V and gives rise to medially directed terminal strands (TS). C and D. Schematic drawings of the terminal strands containing one to six irregularly spaced boutons en passant and terminal boutons (B). DH, dorsal horn.

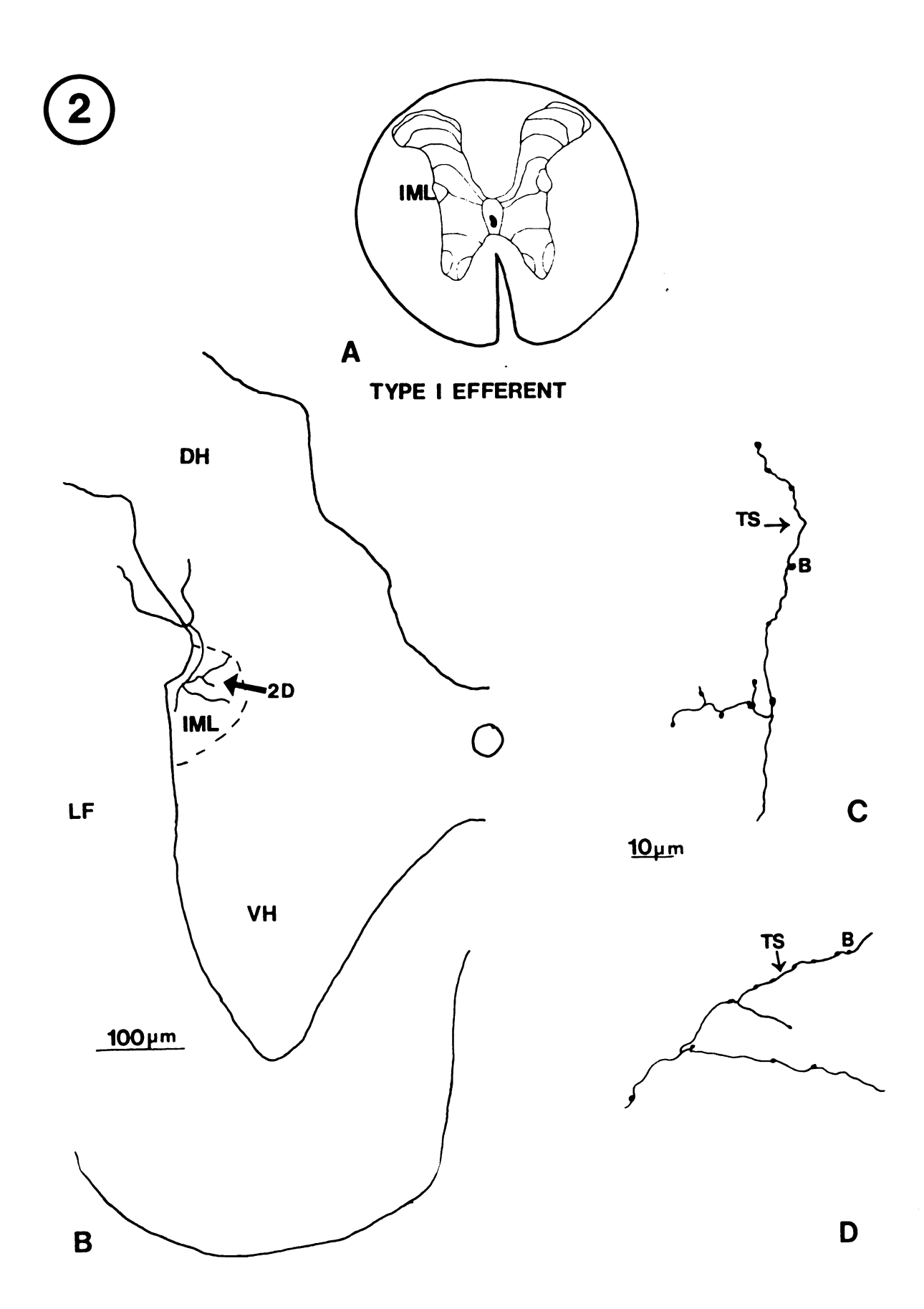


Figure 3: Type II Efferent Axon Terminal Arbors

Composite schematic drawings (A-D) showing the terminal arborization of PHA-L labeled Type II Vo-TS efferent axons in IML of the thoracic spinal cord. A. Thoracic spinal cord laminae. B. A Type II parent fiber traverses the lateral portion of the ventral horn (VH) from the anterior funiculus (AF), enters IML ventrally, and proceeds into the base of the dorsal horn. Within IML the parent fiber gives rise to a collateral which forms a terminal arborization. C. Terminal arborization in IML. Some terminal strands (TS) emanate from the parent fiber (PF) directly. All terminal strands have irregular spaced boutons (B) with a terminal bouton at the end of the strand. D. Terminal arborization in IML. Most terminal strands arise from collateral banches with boutons en passant along their length and terminal boutons at the end of each strand.

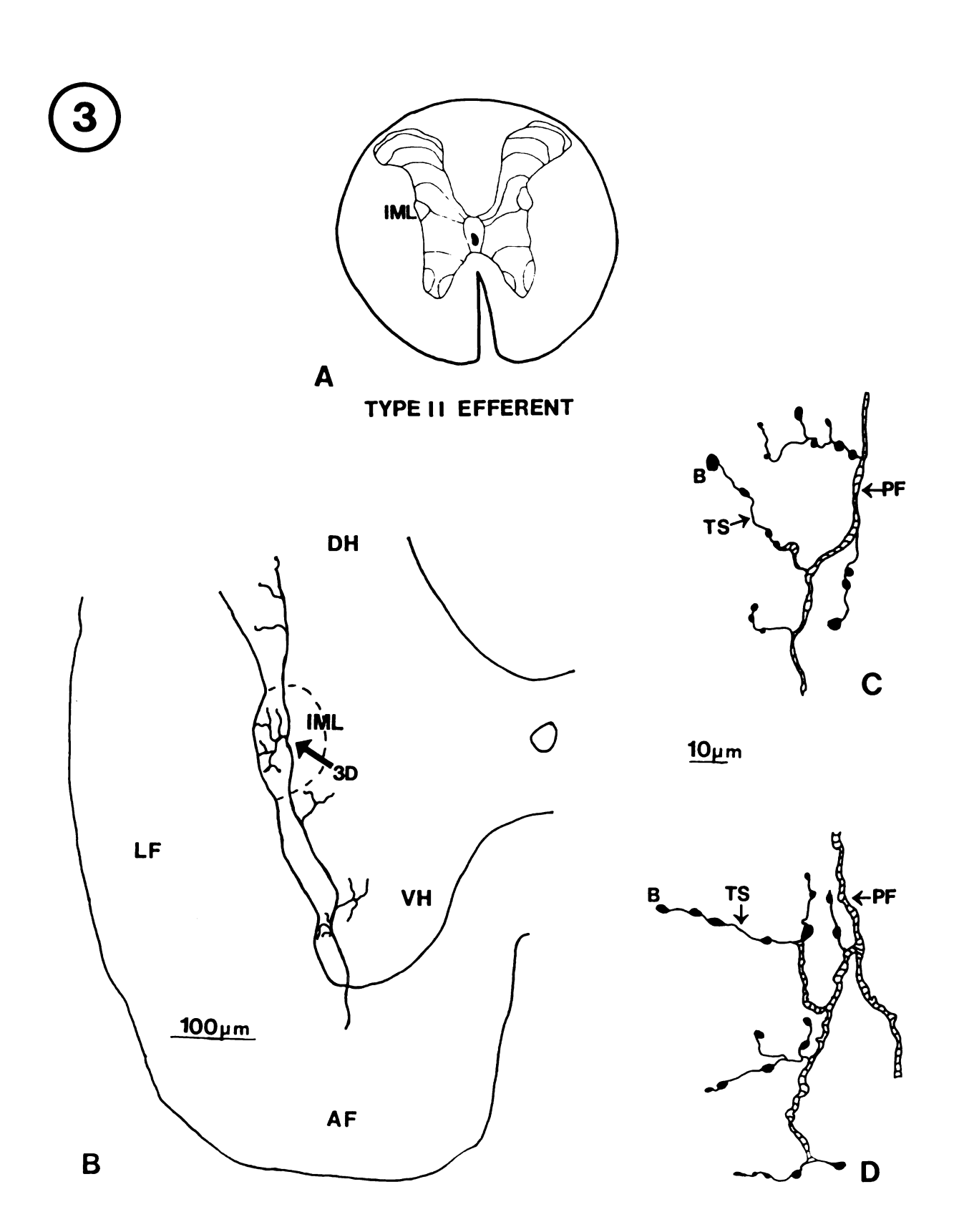
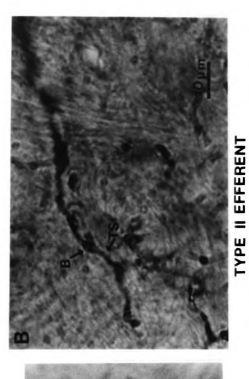


Figure 4: Light Micrographs of Type I and Type II Efferent Axon Terminal Arbors

Photomicrographs (A, B) which document morphological characteristics of Type I (A) and Type II (B) Vo-TS efferent axons terminating in thoracic IML. These photomicrographs highlight the terminal strands (TS) and one bouton (B) each.



B TYPE I EFFERENT



Figure 5: Electron Micrographs of the Cytology and Synaptic Relations of a Type I Efferent Axonal Ending

Adjacent sections (A, B) through an ending (E1) of a Type I Vo-TS efferent axon. This elongated ending has a scalloped contour and forms an asymmetrical to intermediate synaptic junction (arrows) with a dendritic shaft (D). The ending is completely ensheathed by astrocytic processes (AP) except at the presynaptic membrane. X 35,308.

Figure 6: Electron Micrographs of the Cytology and Synaptic Relations of a Type I Efferent Axonal Ending

Adjacent sections (A, B) through an ending (E1) of a Type I Vo-Ts efferent axon. This ending is elongated with a smooth contour and is filled with closely packed agranular spherical synaptic vesicles (40-60 nm in diameter) and a few dense core vesicles (dcv; 85-100 nm in diameter). The ending forms an asymmetrical to intermediate synaptic junction (arrows) with a dendritic shaft (D). The ending is completely ensheathed by astrocytic processes except at the presynaptic membrane. X 35,308.

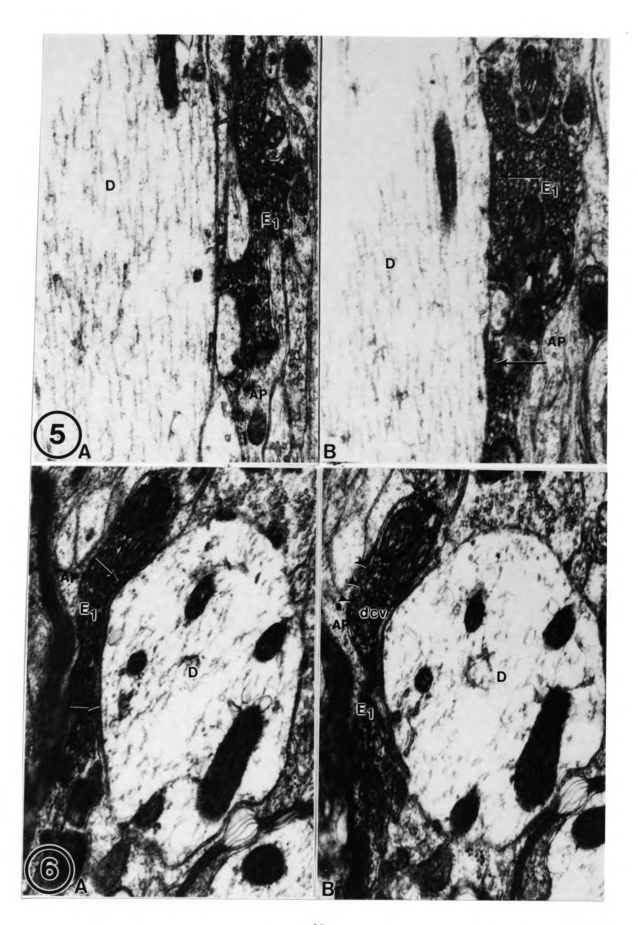


Figure 7 Electron Micrograph of a Type II Parent Axon

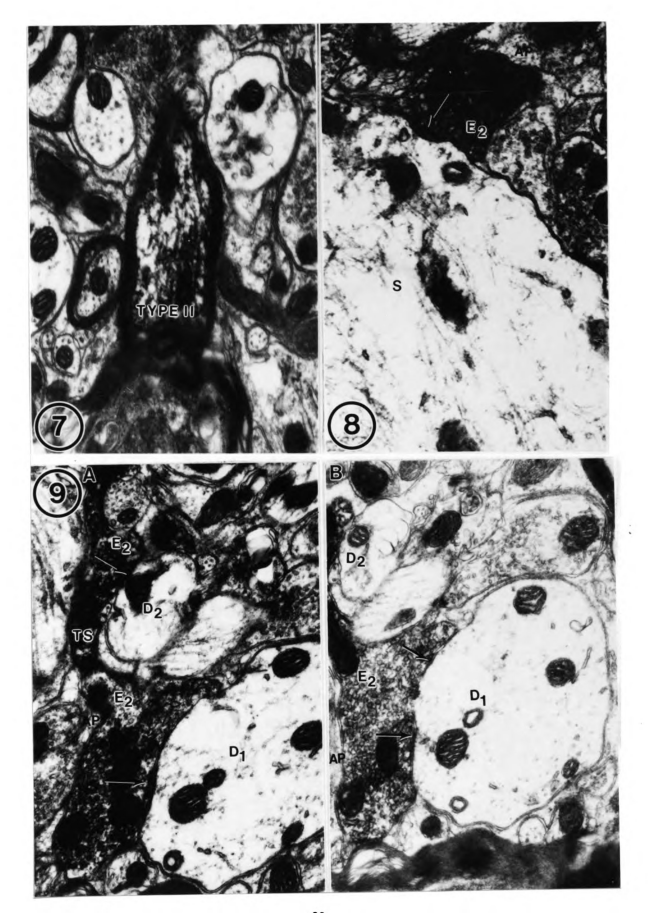
PHA-L labeled parent fiber of a type II Vo-TS efferent axon terminating in thoracic IML. Parent axons are thinly myelinated with a myelin sheath measuring 0.1 to 1.5um in thickness. X 34,920.

Figure 8: Electron Micrograph of the Cytology and Synaptic Relations of a Type II Efferent Axonal Ending

In this electron micrograph a dome-shaped ending (E2) of a Type II Vo-Ts efferent axon forms an intermediate axosomatic synaptic junction (arrow) with a soma (S). The ending contains agranular spherical (40-50 nm in diameter) synaptic vesicles. The ending is ensheathed by an astrocytic process (AP) except at it's presynaptic membrane. X 35,307

Figure 9: Electron Micrographs of the Cytology and Synaptic Relations of Type II Efferent Axonal Endings

Two adjacent sections through two axonal endings (E2) connected by a terminal strand (TS) of a Type II Vo-TS efferent axon. The endings, filled with agranular spherical synaptic vesicles each form asymmetrical to intermediate synaptic junctions (arrows) with a large (D1), and a smaller dendritic (D2) shaft. The endings are ensheathed by astrocytic processes (AP) exept at the presynaptic membrane. X 34,920.



BIBLIOGRAPHY

- 1. Appel, N. M., and R. P. Elde (1988) The interomediolateral cell column of the thoracic spinal cord is comprised of target-specific subnuclei: Evidence from retrograde transport studies and immunohisochemistry. J. Neurosci. 8(5): 1767-1775.
- 2. Arvidsson, J. and Gobel, S. (1978) Further observations of transganglionic degeneration trigeminal primary sensory neurons. Brain Res. 4: 1-12.
- 3. Arvidsson, J. and Gobel, S. (1981) An HRP study of the central projections of primary trigeminal neurons which innervate tooth pulps in the cat. Brain Res. 210: 1-16.
- 4. Azerad, J., Woda, A., and Albe-Fessard, D. (1982) Physiological properties of neurons in different parts of the cat trigeminal sensory complex. Brain Res. 246: 7-21.
- 5. Bowker, R. M., L. C. Abbott, and R. P. Dilts (1988) Peptidergic neurons in the nucleus raphe magnus and the nucleus gigantocellularis: Their distributions, interrelationships, and projections to the spinal cord. Prog. in Brain Res. 77: 95-127.
- 6. Bruce, L. L., J. G. McHaffie and B. E. Stein (1984) Organization of the hamster trigeminal complex: Projections to superior colliculus, thalamus, and spinal cord. Soc. Neurosci. Abstr. 10:483.
- 7. Burton, H. and A. D. Loewy (1976) Descending projections from the marginal cell layer and other regions of the monkey spinal cord. Brain Res. 116:485491.
- 8. Burton. H. and A. D. Jr. Craig, D. A. Poulos, and Molt (1979) Efferent projections from temperature-sensitive recording loci within the marginal zone of the nucleus caudalis of the spinal trigeminal complex of the cat. J. Comp. Neurol. 183: 753-778.
- 9. Burton, H., and A. D. Loewy (1977) Projections to the spinal cord from the medullary somatosensory relay nuclei. J. Comp. Neurol. 173: 773-792.
- Cabana, T. and G. F. Martin (1984) Developmental sequence in the origin of descending spinal pathways. Studies using retrograde transport techniques in the north american opossum (Didelphis virginiana). Dev. Brain Res. 15:247-263.
- 11. Chung, J. M., K. Chung, and R. D. Wurster (1975) Sympathetic preganglionic neurons of the cat spinal cord: Horseradish peroxidase study. Brain Res. 91: 126-131.
- 12. Cliffer, K. D. and G. J. Geisler, Jr. (1988) PHA-L can be transported anterogradely through fibers of passage. Brain Res. 485:185-191.

- 13. Contreras, R. J., R. M. Beckstead and R. Norgren (1982) The central projections of the trigeminal, facial, glossopharyngeal and vagus nerves: An autoradiographic study in the rat. J. Autonomic Ner. Sys. 6:303-322.
- 14. Craig, A. D., Jr. (1978) Spinal and medullary input to the lateral cervical nucleus. J. Comp. Neurol. 181:729-744.
- Crutcher, K. A., A. O. Humbertson and G. F. Martin (1978) The origin of the brainstem-spinal pathways in the north american opossum (Didelphis virginiana). Studies using horseradish peroxidase method. J. Comp. Neurol. 179:169-194
- 16. Darian-Smith, I. (1973) The trigeminal system. In: Handbook of Sensory Physiology. Vol II. A. Iggo, ed. Springer-Verlag, Berlin, pp.271-314.
- 17. Falls, W. M. (1983) Light and EM analysis of identified trigeminospinl projection neurons in rat trigeminal nucleus oralis. Anat. Rec. 205:55A.
- 18. Falls, W. M. (1984a) Termination in trigeminal nucleus oralis of ascending intratrigeminal axons originating from neurons on the medullary dorsal horn:

 An HRP study in the rat employing light and electron microscopy. Brain Res. 290:136-140.
- 19. Falls, W. M. (1983b) A Golgi type II neuron in trigeminal nucleus oralis: A Golgi study in the rat. Neurosci. Letts. 41:11-17.
- 20. Falls, W. M. (1984b) Axonal endings terminating on dendrites of identified large trigeminospinal projection neurons in rat trigeminal nucleus oralis. Brain Res. 324:1279-1298.
- 21. Falls, W. M. (1984c) The morphology of neurons in trigeminal nucleus oralis projecting to the medullary dorsal horn (trigeminal nucleus caudalis): A retrograde horseradish peroxidase and Golgi study. Neuroscience 13:1279-1298.
- 22. Falls, W. M., R. E. Rice, and J. P. Van Wagner (1985) The dorsomedial portion of trigeminal nucleus oralis (Vo) in the rat: Cytology and projections to the cerebellum. Somatosens. Res. 3:89-118.
- 23. Falls, W. M. (1986) Morphology and synaptic connections of myelinated primary axons in the ventrolateral region of the rat trigeminal nucleus oralis. J. of Comp. Neurol. 244:96-110.
- 24. Gerfen, C.R., and P.E. Sawchenko (1984) An anterograde neuroanatomical tracing method that shows the detailed morphology of neurons, their axons and terminals: Immunohistological localization of the axonally transported plant lectin, phaseoulus vulgaris leucoagglutinin (PHA-L). Brain Res. 290:219-238.
- 25. Greenman, P. E. (1996) Principles of manual medicine. 2nd ed. Williams and Wilkins Baltimore, MD pp. 159-172
- 26. Greenwood, F. (1973) An electrophysiological study of the central connections for primary afferent fibers from the dental pulp in the cat. Arch. Oral Biol. 17:701-709.

- 27. Hayashi, H. (1982) Differential terminal distribution of single large cutaneous afferent fibers in the spinal trigeminal nucleus and in the cervical spinal dorsal horn. Brain Res. 244:173-177.
- 28. Hayashi, H., R. Sumino and B. J. Sessle (1984) Functional organization of the trigeminal subnucleus interpolaris: Nociceptive and innocuous afferent inputs, projections to thalamus cerebellum, and spinal cord, and descending modulation from periaqueductal gray. J. Neurophysiol. 51:890-905.
- 29. Jacquin, Mark F. K. Semba, R. W. Rhoades, and M. David Egger (1982)
 Trigeminal primary afferents project bilaterally to dorsal horn and ipsilaterally to cerebellum, reticular formation, and cuneate, solitary, supratrigeminal and vagus nuclei. Brain Res. 246:285-291.
- 30. Jacquin, M. F., K. Semba, M. D. Egger, and R. W. Rhoades (1983) Organization of HRP-labeled trigeminal mandibular primary afferent neurons in the rat. J. Comp. Neurol. 215: 397-420.
- 31. Kuypers, H. G. J. M., and V. A. Maisky (1975) Retrograde axonal transport of horseradish peoxidase from spinal cord to brain stem cell groups in the cat. Neurosci. Letts. 1: 9-14.
- 32. Khayyat, G. F., Yu, Y. J. and King, R. B. (1975) Response patterns to noxious and non-noxious stimuli in rostral trigeminal nuclei. Brain Res. 97: 47-60.
- 33. Leong, S. K., J. Y. Sheih and W. C. Wong(1984) Localizing spinal-cord-projection neurons in adult albino rats. J.Comp. Neurol. 228: 1-17.
- 34. Marfurt, C. F. and D. F. Turner (1984) The central projections of tooth pulp afferent neurons in the rat as determined by the transganglionic transport of horseradish peroxidase. J Comp. Neurol. 223: 525-547.
- 35. Marfurt, C. F. (1981) The central projections of trigeminal primary afferent neurons in the cat as determined by transganglionic transport of horseradish peroxidase. J. Comp. Neurol 223: 535-547.
- 36. Matsushita, M., M. Ikeda, and N. Okado (1982) The cells of origin of the trigeminothalamic, trigeminospinal and trigeminocerebellar projections in the cat. Neuroscience 7: 1439-1454.
- 37. Matsushita, M., N. Okado, M. Ikeda and Y. Hosoya (1980) Identification of spinal projecting neurons in the cat trigeminal spinal and mesencephalic nuclei using the retrograde horseradish peroxidase technique. In: Integrative Control Functions of the Brain, Vol. III. Ito, M., N. Tsukahara, K. Kubota, and K. Yagi (eds.). Amsterdam: Elsevier North Holland Biomedical Press. pp. 161-163.
- 38. Matsushita, M., N. Okado, M. Ikeda and Y. Hosoya (1981) Descending projections form the spinal and mesencephalic nuclei of the trigeminal nerve to the spinal cord in the cat. A study with the horseradish peroxidase technique. J. Comp. Neurol. 196: 173-187.
- 39. Nord, S. G. (1976) Response of neurons in rostral and caudal trigeminal nuclei to tooth pulp stimulation. Brain Res. Bull. 1: 489-492.

- 40. Pannetton, W. M., and Burton, H. (1981) Corneal and periocular representation within the trigeminal sensory complex in the cat studied with transganglionic transport of horseradish peroxidase. J. Comp. Neurol. 199:327-344.
- 41. Petras, J. M., and J. F. Cummings (1972) Autonomic neurons in the spinal cord of the rhesus monkey: A correlation of the findings of cytoarchitectonics and sympathectomy with fiber degeneration following dorsal rhizotomy. J. Comp. Neurol. 146:189-218.
- 42. Petras, J. M., and A. I. Faden (1978) The origin of sympathetic preganglionic neurons in the dog. Brain Res. 144:353-357.
- 43. Ramon y Cajal, S. (1972 reprint) Histologie du Systeme Nerveux de l'Homme et des Vertebres. Vol. I, Instituto Ramon y Cajal, Madrid.
- 44. Rowe, M. J. and Sessle, B. J. (1972) Responses of the trigeminal ganglion and brain stem neurons in the cat to mechanical and thermal stimulation of the face. Brain Res. 42:367-384.
- 45. Ruggiero, D. A., C. A. Ross, and D. J. Reis (1981) Projections from the spinal trigeminal nucleus to the entire length of the spinal cord in the rat. Brain Res. 225:225-233.
- 46. Satoh, K. (1979) The origin of reticulospinal fibers in the rat: A HRP study. J. Hirnforsch. 20:131-332
- 47. Schramm, L. J., J. R. Adair, J. Stribling, and L. Gray (1975) Preganglionic innervation of the adrenal gland of the rat: A study using horseradish peroxidase. Exp. Neurol. 49:540-553.
- 48. Scofield, B. R. (1990) Uptake of phaseoulus vulgaris leucoagglutinin (PHA-L) by axons of passage. J.Neurosci. Methods. 35:47-56.
- 49. Sessle, B. J. and Greenwood, L. F. (1976) Inputs to trigeminal brain stem neurons from facial, oral, tooth pulp and pharyngolaryneal tissue. I. Respnses to innocuous and noxious stimuli. Brain Res. 117:211-226.
- 50. Sessle, B. J. and Hu, J. W. (1981) Raphe -induced suppression of the jaw-opening reflex and single neurons in trigeminal subnucleus oralis, and influence of naloxone and subnucleus caudalis. Pain 10:19-36.
- 51. Shu, S. Y. and G. M. Peterson (1988) Anterograde and retrograde axonal transport of phaseoulus vulgaris leucoagglutinin (PHA-L) from the globus pallidus to the striatum of the rat. J. Neurosci. Meths. 25:175-180.
- 52. Smith, L. A., and W. M. Falls (1988) Efferent projections to rat spinal cord from trigeminal nucleus oralis utilizing the method of PHA-L. Soc. Neurosci. Abstr. 14:697.
- 53. Smith, L. A. and Falls, W. M. (1993) Descending trigeminospinal projections underlying manual manipulations of the head. J. Amer. Osteo. Assoc.94:949.
- 54. Sohn, D. J. and Falls, W. M. (1990) Primary trigeminal axons terminating in the dorsomedial subdivision of rat nucleus oralis. In Michigan Chapter: Society for Neuroscience Abstracts; Vol. XXI.

- 55. Tohyama, M., K. Sakai, M. Touret, D. Salvert, and M. Jouvet (1979) Spinal projections from the lower brain stem in the cat as demonstrated by the horseradish peroxidase technique. II. Projections from the dorsolateral pontine tegmentum and raphe nuclei. Brain Res. 176:215-223.
- 56. Uchizono, K. (1965) Characteristics of excitatory and inhibitory synapses in the central nervous system of the cat. Nature (London) 207:642-643.
- 57. Uchizono, K. (1967) Synaptic organization of the Purkinje cell in the cerebellum of the cat. Exp. Brain Res. 4:97-113.
- 58. Westrum, L. E., Candfield, R. C., and O'Connor, T. A. (1980) Projections from dental structures to the brain stem trigeminal complex as shown by transganglionic transport of horseradish peroxidase. Neurosci. Lett., 20:31-36.
- 59. Westrum, L. E., R. C. Canfield and T. A. O'Connor (1981) Each canine tooth projects to all brain stem trigeminal nuclei in the cat. Exper. Neurol. 74: 787-799.
- 60. Wouterlood, F. G., and H. J. Groenewegen (1985) Neuroanatomical tracing by use of Phaseoulus vulgaris leucoagglutinin (PHA-L): Electron Microscopy of PHA-L filled neuronal somata, dendrites, axons and axon terminals. Brain Res. 326:188-191.

